



AD-A266 427



INSTITUTE REPORT NO. 477

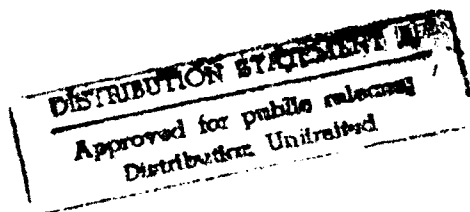
**A MATHEMATICAL MODEL FOR THE STUDY OF HEMORRHAGIC
SHOCK AND FLUID RESUSCITATION:
TRANSCAPILLARY EXCHANGE**

Tammy J. Doherty

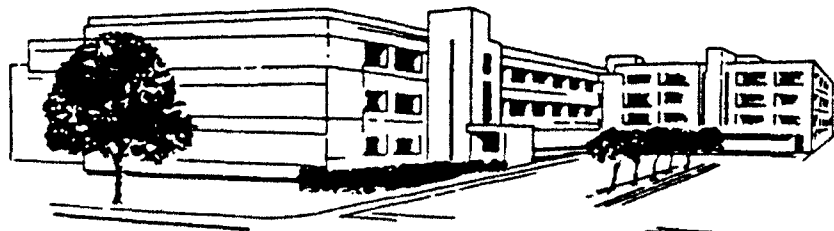
Division of Military Trauma Research



April 1993



93-15221



LETTERMAN ARMY INSTITUTE OF RESEARCH PRESIDIO OF SAN FRANCISCO CALIFORNIA 94129

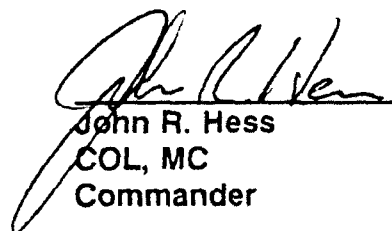
**A MATHEMATICAL MODEL FOR THE STUDY OF HEMORRHAGIC
SHOCK AND FLUID RESUSCITATION: TRANSCAPILLARY EXCHANGE
– Tammy J. Doherty**

**This document has been approved for public release and sale; its
distribution is unlimited.**

**Destroy this report when it is no longer needed. Do not return to the
originator.**

**Citation of trade names in this report does not constitute an official
endorsement or approval of the use of such items.**

**This material has been
reviewed by Letterman Army
Institute of Research and there
is no objection to its
presentation and/or publication.
The opinions or assertions
contained herein are the private
views of the author(s) and are
not to be construed as official
nor as reflecting the views of
the Department of the Army or
the Department of Defense.
(AR 360-5)**

 27 Apr 93
John R. Hess (date)
COL, MC
Commander

REPORT DOCUMENTATION PAGE				Form Approved OMB No 0704-0188	
1a REPORT SECURITY CLASSIFICATION Unclassified			1b RESTRICTIVE MARKINGS		
2a SECURITY CLASSIFICATION AUTHORITY			3 DISTRIBUTION/AVAILABILITY OF REPORT		
2b DECLASSIFICATION/DOWNGRADING SCHEDULE					
4. PERFORMING ORGANIZATION REPORT NUMBER(S) Institute Report No. 477			5. MONITORING ORGANIZATION REPORT NUMBER(S)		
6a. NAME OF PERFORMING ORGANIZATION Letterman Army Institute of Research		6b. OFFICE SYMBOL (If applicable) SGRD-ULT-M	7a. NAME OF MONITORING ORGANIZATION U.S. Army Medical Research and Development Command		
6c. ADDRESS (City, State, and ZIP Code) Letterman Army Institute of Research Division of Military Trauma Research Presidio of San Francisco, CA 94129-6800			7b. ADDRESS (City, State, and ZIP Code) Fort Detrick Fredrick, MD 21701-5012		
8a. NAME OF FUNDING/SPONSORING ORGANIZATION Div. Military Trauma Res.		8b. OFFICE SYMBOL (If applicable) SGRD-ULT-M	9. PROCUREMENT INSTRUMENT IDENTIFICATION NUMBER		
8c. ADDRESS (City, State, and ZIP Code)			10. SOURCE OF FUNDING NUMBERS		
			PROGRAM ELEMENT NO. 61101A	PROJECT NO.	TASK NO. BA
11. TITLE (Include Security Classification) (U) A Mathematical Model for the Study of Hemorrhagic Shock and Fluid Resuscitation: Transcapillary Exchange					
12. PERSONAL AUTHOR(S) Tammy J. Doherty					
13a. TYPE OF REPORT Final		13b. TIME COVERED FROM 1989 TO 1993		14. DATE OF REPORT (Year, Month, Day) March 1993	
15. PAGE COUNT 32					
16. SUPPLEMENTARY NOTATION					
17. COSATI CODES			18. SUBJECT TERMS (Continue on reverse if necessary and identify by block number) model, hemorrhage, fluid resuscitation, transcapillary exchange		
FIELD	GROUP	SUB-GROUP			
19. ABSTRACT (Continue on reverse if necessary and identify by block number) Mathematical models used to predict plasma volume responses to hemorrhage and fluid resuscitation must consider both fluid and solute exchange across the capillary wall. In this paper, we review four models of transcapillary exchange that might be incorporated into a compartmental model for plasma volume prediction. The simplest of the four transcapillary flux models, attributed to Kedem and Katchalsky (1958), assumes a discrete capillary wall structure, ideal solutions, and capillary wall homogeneity. The remaining models become progressively more complex by successive elimination of these three assumptions. To assess their effects on whole-body plasma volume predictions, the four models of transcapillary exchange were incorporated into a simple two-compartment (blood and interstitial space) model. Next, plasma volume predictions were generated for the following simulation conditions: 1) instantaneous 25% loss of blood volume, 2) instantaneous 50% increase in plasma NaCl concentration, 3) instantaneous 50% increase in plasma albumin concentration, and 4) instantaneous 25% loss of blood volume with a 50% increase in plasma NaCl concentration. Plasma volume predictions, generated by the four models, were indistinguishable over these simulation conditions. From these results, we conclude that the simplest of the transcapillary flux models may be used for predicting plasma volume responses to hemorrhage and resuscitative fluid administration.					
20. DISTRIBUTION/AVAILABILITY OF ABSTRACT <input checked="" type="checkbox"/> UNCLASSIFIED/UNLIMITED <input type="checkbox"/> SAME AS RPT. <input type="checkbox"/> DTIC USERS			21. ABSTRACT SECURITY CLASSIFICATION unclassified		
22a. NAME OF RESPONSIBLE INDIVIDUAL John R. Hess, COL, MC Commanding			22b. TELEPHONE (Include Area Code) (415) 561-3600		22c. OFFICE SYMBOL SGRD-JUL7

ABSTRACT

Mathematical models used to predict plasma volume responses to hemorrhage and fluid resuscitation must consider both fluid and solute exchange across the capillary wall. In this paper, we review four models of transcapillary exchange that might be incorporated into a compartmental model for plasma volume prediction. The simplest of the four transcapillary flux models, attributed to Kedem and Katchalsky (1958), assumes a discrete capillary wall structure, ideal solutions, and capillary wall homogeneity. The remaining models become progressively more complex by successive elimination of these three assumptions. To assess their effects on whole-body plasma volume predictions, the four models of transcapillary exchange were incorporated into a simple two-compartment (blood and interstitial space) model. Next, plasma volume predictions were generated for the following simulation conditions: 1) instantaneous 25% loss of blood volume, 2) instantaneous 50% increase in plasma NaCl concentration, 3) instantaneous 50% increase in plasma albumin concentration, and 4) instantaneous 25% loss of blood volume with a 50% increase in plasma NaCl concentration. Plasma volume predictions, generated by the four models, were indistinguishable over these simulation conditions. From these results, we conclude that the simplest of the transcapillary flux models may be used for predicting plasma volume responses to hemorrhage and resuscitative fluid administration.

keywords: model, hemorrhage, fluid resuscitation, transcapillary exchange

ORIGINAL - 100-1008

Accession For	
NTIS GRA&I	<input checked="checked" type="checkbox"/>
DTIC TAB	<input type="checkbox"/>
Unannounced	<input type="checkbox"/>
Justification	
By	
Distribution	
Availability Codes	
Dist	Avail and/or Special
A-1	

A Mathematical Model for the Study of Hemorrhagic Shock and Fluid
Resuscitation: Transcapillary Exchange -- Tammy J. Doherty

INTRODUCTION

One of the most important recovery mechanisms following loss of blood volume is the transfer of fluid across the capillary wall from the interstitium (subscript I) to the capillary (subscript C). According to Starling¹, the forces that govern transcapillary fluid movement are the hydrostatic (P) and osmotic (Π) pressure differences across the capillary wall. Landis² showed that the rate of fluid movement from capillary to interstitium (J_v) is approximately proportional to the difference between these capillary (subscript C) and interstitial (subscript I) pressure differences (Box 1):

$$J_v = k[(P_C - P_I) - (\Pi_C - \Pi_I)] \quad (1)$$

When capillary hydrostatic pressure falls due to loss of blood volume, fluid movement into the capillary space increases, helping restore lost volume. This "autoinfusion" dilutes the blood (lowering osmotic pressure) and causes capillary hydrostatic pressure to increase. Eventually, a new balance of hydrostatic and osmotic forces is reached and transcapillary flux returns to normal levels.

Pre-hospital management of hemorrhagic shock consists of: 1) establishing hemostasis, and 2) replacing lost blood with a fluid substitute. Because whole blood is oftentimes unavailable, lactated Ringer's solution, which has the same osmolarity as normal plasma, is frequently used as a fluid substitute. Fluid and solute components of lactated Ringers solution distribute throughout the interstitial as well as the vascular spaces. Consequently, it takes three or more liters of lactated Ringers solution to replace one liter of shed blood. When large quantities of blood or isosmotic fluid are unavailable, a small volume of a hyperosmotic solution may be used to expand plasma volume using the body's own autoinfusion mechanism. Capillary permeability to the solutes in the resuscitative fluid determines the duration of the osmotic pressure differential across the capillary wall. A hyperosmotic solution made up of highly permeable solutes (e.g., NaCl) will have only a short term effect compared to solutions made up of less permeable solutes (e.g., albumin, dextran, hetastarch), which stay in the blood space longer. For these reasons, the dynamics of

both solute and solvent must be considered when interpreting cardiovascular responses to hemorrhage and fluid resuscitation.

The Landis-Starling Equation (Equation 1) does not account for the permeability of solutes. Transport equations that account for permeability of both solute and solvent generally fall into one of two classes: phenomenologic equations based on irreversible thermodynamics, or mechanical (hydrodynamic) equations based on either "pore" or "matrix" theory. The models in these two classes differ mainly with respect to the definition of model coefficients: the forms of the transport equations are otherwise similar. Consequently, models may be characterized by the simplifying assumptions used in model development, rather than in the theory used to develop equations.

It is difficult to determine, on the basis of model descriptions, which model or set of model assumptions is necessary or sufficient for application to the problem of hemorrhage and fluid resuscitation. The simplest transport model, attributed to Kedem and Katchalsky³ has been criticized because it incorporates assumptions of a thin, homogeneous capillary wall, and ideal solutions made up of small particles. In this paper, we review the Kedem-Katchalsky model as well as other, less restrictive models. The purpose of this endeavor is to identify the simplest model for predicting whole-body, net transcapillary fluid and solute exchange in response to hemorrhage and/or resuscitation fluid administration.

MODEL DESCRIPTIONS

Phenomenologic models based on irreversible thermodynamics were first introduced by Kedem and Katchalsky³ in 1958. The model they developed assumes a homogeneous, discrete membrane structure, and ideal solutions composed of a single type of small solute particle. Several models have been developed to address perceived shortcomings in the Kedem-Katchalsky model. These include a model developed by Patlak⁴ in 1963, which uses a continuous membrane model, as well as Katz' model⁵, developed in 1985, which assumes non-ideal solutions. The basic pore theory model, described by Curry⁶, also incorporates a continuous membrane model and non-ideal solutions. In addition, the pore theory model readily accounts for large solute molecules and multiple pathways for solute and solvent transport. To better understand the effects of model assumptions on flux equations, three models based on irreversible

thermodynamics (i.e., the Kedem-Katchalsky, Patlak, and Katz models), as well as the basic pore theory model, are reviewed below.

The Kedem-Katchalsky Equations

In models based on irreversible thermodynamics, the rate of entropy production (dS/dt) on one side of the membrane is defined in terms of chemical potentials (μ). This equation is then used to generate coupled total volumetric and solute flux equations. Models differ with respect to the form of the entropy production equation (discrete versus continuous) and with respect to simplifying assumptions used in estimating chemical potentials. In the Kedem-Katchalsky model, the rate of entropy production for the interstitial compartment is given by:

$$\frac{dS_I}{dt} = \frac{1}{T} \Delta\mu_w \frac{dN_{w,I}}{dt} + \frac{1}{T} \Delta\mu_s \frac{dN_{s,I}}{dt} \quad (2)$$

where T is temperature, t is time, N is the number of moles of solute (subscript s) or water (subscript w), and the Δ operator represents capillary-interstitial differences. For convenience, the variable Φ is defined as:

$$\Phi = \frac{T dS_I}{A dt} = \Delta\mu_w \dot{n}_w + \Delta\mu_s \dot{n}_s \quad (3)$$

where A is the membrane surface area and \dot{n}_z is defined by:

$$\dot{n}_z = \frac{1}{A} \frac{dN_{z,I}}{dt} \quad (4)$$

For an ideal solution, the chemical potential difference (μ) is defined in terms of hydrostatic pressures (P), molar volumes (V), and partial molar fractions (γ):

$$\Delta\mu = V\Delta P + RT\Delta\ln(\gamma) \quad (5)$$

where R is the universal gas constant and the partial molar solute fraction is defined by:

$$\gamma_s = \frac{n_s}{n_s + n_w} \quad (6)$$

Assuming a dilute, binary solution, (i.e., $n_s \ll n_w$ and $n_s + n_w \approx n_w$), γ_s may be approximated by the term (n_s/n_w) and solute concentration (C_s) by the term $(n_s/V_w n_w)$. Using these approximations, $\Delta\ln(C_s)$ may be substituted

for $\Delta \ln(\gamma_s)$ in Equation 5, and the solute chemical potential difference across the membrane becomes:

$$\Delta \mu_s = V_s \Delta P + RT \Delta \ln(C_s) \quad (7)$$

In their paper³, Kedem and Katchalsky rewrite Equation 7 in the following form:

$$\Delta \mu_s = V_s \Delta P + RT \frac{\Delta C_s}{\hat{C}_s} \quad (8)$$

where \hat{C} is defined by:

$$\hat{C}_s = \frac{\Delta C_s}{\Delta \ln(C_s)} \quad (9)$$

To determine the corresponding equation for the water or solvent chemical potential difference, $\ln(\gamma_w)$ is represented by $\ln(1-\gamma_s)$ which, for small γ_s , is approximately equal to $-\gamma_s$. Again assuming dilute, binary solutions (i.e., $n_s + n_w \approx n_w$ and $C_s \approx n_s/V_w n_w$), the expression for the water chemical potential difference becomes:

$$\Delta \mu_w = V_w \Delta P - RT V_w \Delta C_s \quad (10)$$

Substituting the definitions of $\Delta \mu_s$ and $\Delta \mu_w$ from Equations 8 and 10 into Equation 3 and rearranging terms yields:

$$\Phi = (\dot{n}_w V_w + \dot{n}_s V_s) \Delta P + \left(\frac{\dot{n}_s}{\hat{C}_s} - \dot{n}_w V_w \right) RT \Delta C_s \quad (11)$$

Equation 11 may be simplified by adding and subtracting the term $\dot{n}_s V_s RT \Delta C_s$, by substituting J_v for the term $(\dot{n}_s V_s + \dot{n}_w V_w)$, and substituting $\Delta \Pi$ for the term $(RT \Delta C_s)$:

$$\Phi = J_v (\Delta P - \Delta \Pi) + J_s V_s \left(1 + \frac{1}{\hat{C}_s V_s} \right) \Delta \Pi \quad (12)$$

By the rules of irreversible thermodynamics⁷, any equation for the rate of entropy generation of the form of Equation 12 (i.e., sums of fluxes

multiplied by their own driving forces) may be recast in the form of exact coupled flux equations as follows:

$$J_v = L_{11}(\Delta P - \Delta \Pi) + L_{12} \left(1 + \frac{1}{\hat{C}_s V_s} \right) \Delta \Pi \quad (13)$$

$$J_s V_s = L_{21}(\Delta P - \Delta \Pi) + L_{22} \left(1 + \frac{1}{\hat{C}_s V_s} \right) \Delta \Pi \quad (14)$$

An expression for $(\Delta P - \Delta \Pi)$ may be obtained from Equation 13 and substituted into Equation 14 to yield:

$$J_s V_s = \frac{L_{21}}{L_{11}} \left(J_v - L_{12} \left(1 + \frac{1}{\hat{C}_s V_s} \right) \Delta \Pi \right) + L_{22} \left(1 + \frac{1}{\hat{C}_s V_s} \right) \Delta \Pi \quad (15)$$

By assuming that $L_{12} = L_{21}$ (Onsager's reciprocity law), that $\Delta \Pi = RT \Delta C_s$ (van't Hoff's law for ideal solutions), and that $\hat{C}_s V_s \approx 0$ for small particles in dilute solution, Equations 13 and 15, after rearranging terms, become:

$$J_v = k_v [\Delta P - \sigma \Delta \Pi] \quad (16)$$

$$J_s = k_s \Delta C_s + (1 - \sigma) J_v \hat{C}_s \quad (17)$$

where:

$$k_v = L_{11} \quad (18)$$

$$\sigma = 1 - \frac{L_{12}}{L_{11}} \left(1 + \frac{1}{\hat{C}_s V_s} \right) \quad (19)$$

$$k_s = \frac{RT}{V_s} \left(L_{22} - \frac{L_{12}^2}{L_{11}} \right) \left(1 + \frac{1}{\bar{C}_s V_s} \right) \quad (20)$$

Equation 16 is similar to the Landis-Starling Equation (Equation 1) but includes an "osmotic reflection coefficient" (σ), defined as the fraction of the osmotic pressure, that would be manifest across an ideal, semipermeable membrane, that is manifest across the non-ideal capillary wall⁸. From this definition, $\sigma=1$ when the membrane is impermeable to solute, and $\sigma=0$ when the membrane is highly permeable to solute. A summary of the Kedem-Katchalsky Equations, extended for a system of multiple, non-interacting solutes, is presented in Box 2.

The Patlak (nonlinear) Equations

A major assumption used in the Kedem-Katchalsky formulation is that the capillary wall is thin enough to represent pressure and concentration gradients in discrete form. This assumption has been shown to be invalid unless the rate of solvent flux is very small^{4,9-11}. Patlak⁴ was the first to reformulate the solute and solvent flux equations using a continuous membrane model:

$$J_v = k_v w \left[\frac{dP}{dx} - \sigma \frac{d\Pi}{dx} \right] \quad (21)$$

$$J_s = -k_s w \frac{dC_s}{dx} + (1-\sigma) J_v C_s \quad (22)$$

where x is a point along the transport pathway, and w is the total distance across the capillary/interstitial membrane. Assuming that k_v , k_s , and σ are constant (i.e., independent of C_s and x), and that a steady state is obtained (i.e., J_s and J_v are independent of time and distance, x), then integration of Equations 21 and 22 leads to the following solutions for J_v and J_s :

$$J_v = k_v (\Delta P - \sigma \Delta \Pi) \quad (23)$$

$$J_s = (1-\sigma) J_v \frac{(C_{s,c} - C_{s,i} e^{-Pe})}{(1 - e^{-Pe})} \quad (24)$$

where Pe , a form of the Peclet number, is defined as:

$$Pe = \frac{(1 - \sigma) J_v}{k_s} \quad (25)$$

Equations 23-25, extended to a system of multiple, non-interacting solutes, are presented in Box 3.

Equations for non-ideal solutions

Both the Kedem-Katchalsky and Patlak equations assume that the solutions on the two sides of the membrane are ideal. Katz⁵ rederived the transport equations using a continuous membrane model, assuming non-ideal solutions. As in the Kedem-Katchalsky derivation, Katz begins his derivation by defining a variable Φ which is the rate of entropy production multiplied by temperature and divided by membrane area. Because Katz assumes a continuous membrane, the expression for Φ differs somewhat from the expression used by Kedem and Katchalsky (see Equation 3):

$$\Phi = \frac{T}{A} \frac{dS}{dt} = \dot{n}_w \frac{d\mu_w}{dx} + \dot{n}_s \frac{d\mu_s}{dx} \quad (26)$$

where \dot{n} is defined as in Equation 4. Katz uses a general expression for chemical potential:

$$\mu = VP + RT \ln(a) \quad (27)$$

in which a is the "chemical species activity", rather than the more restrictive definition used by Kedem and Katchalsky (Equations 5-10). Taking the differential of both sides of Equation 27, it is possible to write:

$$\frac{d\mu_s}{dx} = V_s \frac{dP}{dx} + RT \frac{d\ln(a_s)}{dx} \quad (28)$$

$$\frac{d\mu_w}{dx} = V_w \frac{dP}{dx} + RT \frac{d\ln(a_w)}{dx} \quad (29)$$

Substituting these definitions of $d\mu_s/dx$ and $d\mu_w/dx$ into Equation 26 and rearranging terms yields:

$$\Phi = (\dot{n}_w V_w + \dot{n}_s V_s) \frac{dP}{dx} + \left(\dot{n}_s \frac{d\ln(a_s)}{dx} + \dot{n}_w \frac{d\ln(a_w)}{dx} \right) RT \quad (30)$$

Adding and subtracting the term:

$$\frac{\dot{n}_s V_s RT}{V_w} \frac{d\ln(a_w)}{dx} \quad (31)$$

to and from the right side of equation 30, substituting J_v for the term $(\dot{n}_s V_s + \dot{n}_w V_w)$, substituting J_s for the term (\dot{n}_s) , and regrouping terms yields:

$$\Phi = J_v \left[\frac{dP}{dx} + \frac{RT}{V_w} \frac{d\ln(a_w)}{dx} \right] + J_s V_s \left(\frac{RT}{V_s} \frac{d\ln(a_s)}{dx} - \frac{RT}{V_w} \frac{d\ln(a_w)}{dx} \right) \quad (32)$$

In an isothermal, noncontractile, isoelectric system with N_w moles of water and N_s moles of solute, the Gibbs-Duhem equation⁵ states:

$$-VdP + \sum N_i d\mu_i = 0 \quad (33)$$

or, in the present case:

$$-(n_w V_w + n_s V_s) dP + n_w [V_w dP + RT d\ln(a_w)] + n_s [V_s dP + RT d\ln(a_s)] = 0 \quad (34)$$

The dP terms in Equation 34 drop out, leaving an expression for $d\ln(a_s)$ as a function of $d\ln(a_w)$:

$$d\ln(a_s) = -\frac{n_w}{n_s} d\ln(a_w) \quad (35)$$

Substituting this expression for $d\ln(a_s)$ into Equation 32 and rearranging terms yields:

$$\Phi = J_v \left[\frac{dP}{dx} + \frac{RT}{V_w} \frac{d\ln(a_w)}{dx} \right] + J_s V_s \left(1 + \frac{n_w V_w}{n_s V_s} \right) \left(\frac{-RT}{V_w} \frac{d\ln(a_w)}{dx} \right) \quad (36)$$

Katz defines the osmotic pressure differential as the hydrostatic pressure gradient that must be applied to a system to maintain that system in equilibrium when a chemical potential gradient exists⁵:

$$\frac{d\Pi}{dx} = - \frac{RT}{V_w} \frac{d \ln(a_w)}{dx} \quad (37)$$

Using this definition, we may rewrite the expression for Φ (Equation 36) in terms of Π :

$$\Phi = J_v \left(\frac{dP}{dx} - \frac{d\Pi}{dx} \right) + J_s V_s \left(1 + \frac{n_w V_w}{n_s V_s} \right) \frac{d\Pi}{dx} \quad (38)$$

By the rules of irreversible thermodynamics⁷, any equation for the rate of entropy generation of the form of Equation 38 (i.e., sums of fluxes multiplied by their own driving forces) may be recast in the form of exact coupled flux equations as follows:

$$J_v = L_{11} \left(\frac{dP}{dx} - \frac{d\Pi}{dx} \right) + L_{12} \left(1 + \frac{n_w V_w}{n_s V_s} \right) \frac{d\Pi}{dx} \quad (39)$$

$$J_s V_s = L_{21} \left(\frac{dP}{dx} - \frac{d\Pi}{dx} \right) + L_{22} \left(1 + \frac{n_w V_w}{n_s V_s} \right) \frac{d\Pi}{dx} \quad (40)$$

Using the same procedures as in the Kedem-Katchalsky derivation, these equations may be simplified to:

$$J_v = k_v w \left[\frac{dP}{dx} - \sigma \frac{d\Pi}{dx} \right] \quad (41)$$

$$J_s = \alpha_1 w \frac{d\Pi}{dx} + \alpha_2 J_v \quad (42)$$

where:

$$k_v = \frac{L_{11}}{w} \quad (43)$$

$$\sigma = 1 - \frac{L_{12}}{L_{11}} \left(1 + \frac{n_w V_w}{n_s V_s} \right) \quad (44)$$

$$\alpha_1 = \frac{1}{V_s w} \left(L_{22} - \frac{L_{12}^2}{L_{11}} \right) \left(1 + \frac{n_w V_w}{n_s V_s} \right) \quad (45)$$

$$\alpha_2 = \frac{L_{12}}{L_{11} V_s} \quad (46)$$

The solution for Equation 41 is straightforward and is identical to the Patlak solution (Equation 23). To solve Equation 42, Katz⁵ rewrites the equation in terms of solute concentration, using a third order polynomial to express osmotic pressure as a function of solute concentration:

$$\Pi = a_1 C_s + a_2 C_s^2 + a_3 C_s^3 \quad (47)$$

Taking the derivative of both sides of Equation 47 with respect to C_s , results in the following relationship between $d\Pi$ and dC_s :

$$d\Pi = (a_1 + 2a_2 C_s + 3a_3 C_s^2) dC_s \quad (48)$$

Katz substitutes this expression for $d\Pi$ into Equation 42, resulting in the following expression for J_s in terms of C_s :

$$J_s = \alpha_1 w (a_1 + 2a_2 C_s + 3a_3 C_s^2) \frac{dC_s}{dx} + \alpha_2 J_v \quad (49)$$

to solve this equation, Katz assumes that the α_1 term is concentration-dependent:

$$\alpha_1 = 1 + \frac{\alpha_3}{C_s} \quad (50)$$

and that the α_2 term is concentration-independent. Using these assumptions, it is possible to solve Equation 49:

$$J_s = [b_0 \Delta(\ln(C_s)) + b_1 \Delta(C_s) + b_2 \Delta(C_s^2) + b_3 \Delta(C_s^3)] + \alpha_2 J_v \quad (51)$$

where, the b_i terms are functions of α_3 and a_i terms, and as before, the symbol Δ represents capillary-interstitial differences.

Unfortunately, the assumptions of constant α_1 and concentration-dependent α_2 , used to solve Equation 49, contradict accepted notions of concentration independence for the coefficient of diffusion (related to α_1) and concentration-dependence of the convective transport coefficient (α_2), which is usually represented by the product of the solute concentration (C_s), and a "slip" coefficient (e.g., $1-\sigma$ in the Kedem-Katchalsky solution). Because there is no apparent basis for the assumptions used by Katz, an alternative solution is presented below.

To begin, an expression for J_s is derived from Equations 39 and 40 using the coefficients ω and σ :

$$J_s = -\omega w \frac{d\Pi}{dx} + (1-\sigma) J_v C_s \quad (52)$$

where:

$$\omega = \frac{1}{w V_s} \left(\frac{L_{12}^2}{L_{11}} - L_{22} \right) \left(1 + \frac{n_w V_w}{n_s V_s} \right) \quad (53)$$

and σ is defined as in Equation 44. Substituting the expression for $d\Pi$ from Equation 48 into Equation 52, and solving the resulting differential equation yields the following equation relating solute concentration, solute flux, and total volumetric flux:

$$\left(a_1 + \frac{2a_2 J_s}{b} + \frac{3a_3 J_s^2}{b^2} \right) \ln \left| \frac{C_{s,i} - \frac{J_s}{b}}{C_{s,c} - \frac{J_s}{b}} \right| + 2a_2 \Delta C_s + 3a_3 \Delta C_s \left[\bar{C}_s + \frac{J_s}{b} \right] = \frac{b}{\omega} \quad (54)$$

where:

$$b = (1 - \sigma) J_v \quad (55)$$

$$\bar{C}_s = \frac{C_{s,c} + C_{s,l}}{2} \quad (56)$$

An approximate solution for J_s from Equation 54 may be obtained using numerical search techniques. The new non-ideal flux equations (i.e., Equations 41 and 54), extended to a system of multiple, non-interacting solutes, are presented in Box 4.

Pore Theory

The first discussion of pore theory is attributed to J.R. Pappenheimer¹². Since that time, numerous descriptions of hydrodynamic flow through pores traversing the capillary wall have been published. In this review, we assume that both water and solutes (approximated by rigid spheres) are transported across the capillary wall through cylindrical pores. The conceptual model by Anderson and Malone¹³ (Figure 1) is used to estimate both solvent and solute flux through these pores. The distance from the center of the pore to the wall is r_p , and the radius of the solute molecule is r_s . To determine the solute concentration at any location within the pore, the centers of the solute molecules, within the region bounded by $x + \Delta x$, are counted. Because the solute molecules are of finite size, the centers of the molecules are prohibited from the region adjacent to the pore wall. Thus, the capillary pore may be divided into a zone near the pore axis (i.e., the "core region"), in which solute is free to move ($0 < r \leq r_p - r_s$), and a zone near the pore wall (the "exclusion region"), in which the solute concentration is zero ($r_p - r_s < r < r_p$).

A key assumption in this model is that of radial equilibrium. Hydrostatic and osmotic pressure gradients are assumed not to exist in the radial (r) direction except across the imaginary boundary at $r = r_p - r_s$. Thus, the hydrostatic and osmotic pressures at any point in the "core" region, at distance x along the pore, may be expressed by the hydrostatic and osmotic pressures at the pore axis ($P(x)$ and $\Pi(x)$, respectively). Because the solute concentration in the exclusion region is zero, the osmotic pressure in that region must also be zero. Across the imaginary boundary at $r = r_p - r_s$, the driving force for solvent flow is the difference between hydrostatic and osmotic pressures. Therefore, the hydrostatic pressure in the exclusion region equals $P(x) - \Pi(x)$.

Using these results, i.e., that the hydrostatic pressure in the core region is $P(x)$, and the hydrostatic pressure in the exclusion region is $[P(x) - \Pi(x)]$, it is possible to write simplified Navier-Stokes Equations for the core and exclusion regions, separately:

$$\frac{dP}{dx} = \frac{\eta}{r} \frac{d}{dr} \left(r \frac{dv}{dr} \right), \quad 0 \leq r \leq r_p - r_s \quad (57)$$

$$\frac{dP}{dx} - \frac{d\Pi}{dx} = \frac{\eta}{r} \frac{d}{dr} \left(r \frac{dv}{dr} \right), \quad r_p - r_s < r \leq r_p \quad (58)$$

where η is fluid viscosity. By separating Equation 58 into hydrostatic (subscript P) and osmotic (subscript Π) pressure components:

$$\frac{dP}{dx} = \frac{\eta}{r} \frac{d}{dr} \left(r \frac{dv_P}{dr} \right), \quad r_p - r_s \leq r \leq r_p \quad (59)$$

$$-\frac{d\Pi}{dx} = \frac{\eta}{r} \frac{d}{dr} \left(r \frac{dv_{\Pi}}{dr} \right), \quad r_p - r_s < r \leq r_p \quad (60)$$

it is possible to generate equations (using Equations 57, 59, and 60) that describe the effects of hydrostatic pressure over the entire pore region (Equation 61), and osmotic pressure in the exclusion region (Equation 62):

$$\frac{dP}{dx} = \frac{\eta}{r} \frac{d}{dr} \left(r \frac{dv_P}{dr} \right), \quad 0 \leq r \leq r_p \quad (61)$$

$$-\frac{d\Pi}{dx} = \frac{\eta}{r} \frac{d}{dr} \left(r \frac{dv_{\Pi}}{dr} \right), \quad r_p - r_s < r \leq r_p \quad (62)$$

The solute velocity due to hydrostatic pressure may be obtained by integrating Equation 61 twice with respect to r , applying the boundary conditions: 1) $dv_P/dr = 0$ at $r=0$, and 2) $v_P=0$ at $r=r_p$:

$$v_p = \frac{(r^2 - r_p^2)}{4\eta} \frac{dP}{dx} \quad (63)$$

Similarly, velocity due to osmotic pressure in the exclusion region may be obtained by integrating Equation 62 twice with respect to r , applying the boundary conditions: 1) $v_{\Pi} = 0$ at $r = r_p - r_s$ and 2) $v_{\Pi} = 0$ at $r = r_p$:

$$v_{\Pi} = \frac{-(r^2 - r_p^2)}{4\eta} \frac{d\Pi}{dx} + \frac{(r_p - r_s)^2}{2\eta} \frac{d\Pi}{dx} [\ln(r) - \ln(r_p)] \quad (64)$$

The solvent flow through the pore ($J_{v,p}$) is obtained by integrating each velocity term over the appropriate pore area:

$$J_{v,p} = \int_0^{r_p} v_p 2\pi r dr + \int_{r_p - r_s}^{r_p} v_{\Pi} 2\pi r dr \quad (65)$$

Solving these integrals and grouping terms yields an expression for solvent flux in terms of pressure gradients, and pore and solvent radii:

$$J_{v,p} = \frac{\pi r_p^4}{8\eta} \left[\frac{dP}{dx} - (1 - (1 - \lambda)^2)^2 \frac{d\Pi}{dx} \right] \quad (66)$$

where $\lambda = r_s/r_p$. Equation 66 may be expressed using the coefficient: k_v and σ as follows:

$$J_v = k_v w \left[\frac{dP}{dx} - \sigma \frac{d\Pi}{dx} \right] \quad (67)$$

where:

$$k_v = \frac{\pi r_p^4}{8\eta w} \quad (68)$$

$$\sigma = (1 - (1 - \lambda)^2)^2 \quad (69)$$

The volumetric flux equation, extended to a solution of multiple, non-interacting solutes, is presented in Box 5.

Equations describing solute flux through capillary pores use the same geometric model as that used to describe solvent flux (Figure 1). For

simplicity, total solute flux is divided into pure-diffusion and pure-convection components. To determine the rate of pure solute diffusion (assuming solvent flux is zero), a small cross section of the pore, of thickness dx , is considered⁶ (Figure 2). Because the centers of the solute molecules are restricted from the area close to the pore walls, the effective area for diffusion ($A_{s,p}$) includes the central area of the pore out to a radius of $r_p - r_s$. The cross-section is considered to be bounded upstream and downstream by semipermeable membranes. A difference in solute concentration across the section leads to a difference in osmotic pressure ($d\Pi$). If unopposed, this osmotic pressure gradient causes water to flow from one side of the section to the other. In a closed system, this osmotic pressure gradient is associated with movement of the cross section in the opposite direction. To prevent movement of the segment and to maintain the osmotic pressure gradient, a force must be exerted on the segment contents to prevent osmotic flow. Thus, each solute molecule within the section is considered to be acted upon by a pressure force (F_Π) of magnitude:

$$F_\Pi = \frac{d\Pi}{N_A C_s dx} \quad (70)$$

where the solute concentration within the section is C_s , and N_A is Avagadro's Number. In a system with constant velocity, this force must be balanced by the drag on the solute molecule caused by solute-solvent interactions and interaction with the pore wall. Faxen¹⁴ determined that the appropriate drag force, which accounts for the presence of the pore wall is:

$$F_D = \frac{-6\pi\eta r_s v_s}{f_{s,p}} \quad (71)$$

where $-6\pi\eta r_s v_s$ is the Stoke's drag force for a sphere in an unbounded fluid, and $f_{s,p}$ is a correction coefficient for the presence of the pore walls:

$$f_{s,p} = 1 - 2.104433\lambda + 2.08877\lambda^3 - 0.94813\lambda^5 - 1.372\lambda^6 + 3.87\lambda^8 - 4.19\lambda^{10} \quad (72)$$

At constant velocity, F_Π equals F_D . Setting the right side of Equation 70 equal to the right side of Equation 71 and solving for v_s yields an expression for solute velocity when volumetric flow is zero (i.e., pure diffusion):

$$v_{s,diff} = \left(\frac{-f_{s,p}}{N_A C_s 6\pi \eta r_s} \right) \frac{d\Pi}{dx} \quad (73)$$

Total solute flux due to diffusion for the single pore ($J_{s,diff}$) is obtained by multiplying $v_{s,diff}$ by the number of moles of solute at the pore cross-section ($C_s \pi(r_p - r_s)^2$). After simplification, $J_{s,diff}$ is expressed by:

$$J_{s,diff} = \pi (r_p - r_s)^2 \left(\frac{-f_{s,p}}{N_A 6\pi \eta r_s} \right) \frac{d\Pi}{dx} \quad (74)$$

To determine the rate of pure convective solute transport (assuming concentration gradients equal zero) in a single pore, we assume that the center of a neutrally buoyant sphere, suspended in a Poiseuillian flow, translates along a streamline of the undisturbed flow¹⁵. The velocity of such a solute molecule, located at a distance r from the pore axis, is the same as the Poiseuille fluid velocity (v_f) at that point:

$$v_{s,conv}(r) = v_f(r) = 2 \left(1 - \frac{r^2}{r_p^2} \right) \bar{v}_f \quad (75)$$

where \bar{v}_f is the average fluid velocity within the pore cross-section. Convective solute flux for the pore is obtained by integrating solute velocity over the pore area bounded by $r=0$ and $r=r_p - r_s$, and multiplying by solute concentration:

$$J_{s,conv} = C_s \int_0^{r_p - r_s} v_{s,conv} 2\pi r dr \quad (76)$$

Substituting the right side of Equation 75 for $v_{s,conv}$, solving the integral and simplifying terms yields an expression for the convective solute transport in a single pore:

$$J_{s,conv} = C_s \bar{v}_f \pi r_p^2 (1 - \lambda)^2 [2 - (1 - \lambda)^2] \quad (77)$$

where, again, λ is r_s/r_p .

Total solute flux (convection plus diffusion) for a single pore is obtained by adding Equations 74 and 77, substituting $A_{s,p}$ for the term $\pi(r_p - r_s)$, and substituting J_v for the term $\bar{v}_f \pi r_p^2$:

$$J_{s,p} = A_{s,p} \left(\frac{-f_{s,p}}{N_A 6 \pi \eta r_s} \right) \frac{d\Pi}{dx} + C_s J_v (1-\lambda)^2 [2 - (1-\lambda)^2] \quad (78)$$

Equation 78 may be rewritten in a form similar to the non-ideal solute transport equation (Equation 52) by regrouping terms:

$$J_{s,p} = -\omega w \frac{d\Pi}{dx} + \chi C_s J_{v,p} \quad (79)$$

where:

$$\omega = A_{s,p} \left(\frac{f_{s,p}}{N_A 6 \pi \eta r_s w} \right) \quad (80)$$

$$\chi = (1 - \lambda)^2 [2 - (1 - \lambda)^2] \quad (81)$$

The solute transport equation, for a solution of multiple solutes, is presented in Box 5.

MODEL COMPARISONS

The choice of model equations for transcapillary flux depends upon the application. Although the Kedem-Katchalsky model has been criticized as being too simplistic, this criticism may not apply to studies of whole-body net transcapillary flux. To assess the effects of different model assumptions on predictions of plasma volume response to hemorrhage and fluid resuscitation, a simple two compartment model was devised. Constants and initial conditions for this model are provided in Table 1. Model compartments, representing the vascular and interstitial fluid spaces, were considered compliant and well-mixed. Hydrostatic pressures were estimated from compartment volumes as follows:

$$P_C = 0.91(V_B - V_{B_0}) + P_{C_0} \quad (82)$$

$$P_I = 0.01042(V_I - V_{I_0}) + P_{I_0} \quad (83)$$

where V_B is the total blood volume, V_I is interstitial volume, and the subscript 0 denotes initial values. For simplicity, it was assumed that plasma and interstitial fluids were made up of water, NaCl, albumin, and globulin. At body temperature, the osmotic pressure for NaCl (subscript s) is approximately:

$$\Pi_s = (31.877)(19330)C_s \quad (84)$$

where C_s is the concentration of NaCl (g/ml), 31.877 converts grams of NaCl to milliosmoles, and 19.33×10^3 is the osmotic pressure (mm Hg) exerted by 1 mosm/ml of solute¹⁶. Cubic equations presented by Landis and Pappenheimer¹⁷ are used to estimate partial osmotic pressures for albumin (subscript a) and globulin (subscript g):

$$\Pi_a = 280C_a + 1800C_a^2 + 12000C_a^3 \quad (85)$$

$$\Pi_g = 210(C_a + C_g) + 1600(C_a + C_g)^2 + 9000(C_a + C_g)^3 - \Pi_a \quad (86)$$

where C_a is albumin concentration (g/ml) and C_g is globulin concentration (g/ml).

Fluid, NaCl, and albumin exchange between the blood and interstitial compartments was assumed to occur across the capillary wall, as well as by lymph return (transport of globulin was neglected). Parameter values for the flux equations were obtained by requiring that at normal steady-state, total volumetric flux is equivalent to lymph return ($0.02 \text{ ml} \cdot \text{kg}^{-1} \cdot \text{min}^{-1}$), and that total solute flux is equivalent to convective solute transport in lymph (interstitial concentration multiplied by normal lymph flow rate). In addition, for models based on irreversible thermodynamics, solute reflection coefficients were assumed to equal the values provided in Table 2. Initial parameter values for the pore theory model were based on reported values for solute¹⁸ and pore¹⁹ radii identified in Table 3.

Because pore theory parameter values were not comparable to parameter values for the models based on irreversible thermodynamics, it was necessary to run two sets of comparisons. In the first set, we

compared predictions generated by the three models based on irreversible thermodynamics. There was no appreciable difference between predictions generated by these three models in response to a simulated instantaneous a) 25% loss of blood volume, b) 50% increase in plasma NaCl concentration, c) 50% increase in plasma albumin concentration, or d) 25% loss of blood volume with a 50% increase in plasma NaCl concentration (Figure 3). Therefore, it was concluded that considerations of membrane continuity and solution non-ideality are unimportant in predictions of whole-body plasma volume response to changes in blood volume or plasma osmolarity.

The second set of comparisons included a discrete, ideal form of a two-pore hydrodynamic model (Box 6) and a two-pore parameter-averaged model, identical in form to the Kedem-Katchalsky model (Box 2). Parameter values for the two-pore model are provided in Table 3. Averaged parameter values are provided in Table 4. The two models generated nearly identical predictions of plasma volume for simulation conditions a) through d), above (Figure 4). These results indicate that the effects of capillary wall nonhomogeneity may be accounted for using a simple, parameter-averaged, phenomenologic model.

The response of the two-pore model to simulated changes in plasma solute concentration or total blood volume (Figure 4) is much slower than that predicted by models based on irreversible thermodynamics (Figure 3) or that observed under laboratory conditions²⁰. Modification of pore sizes ($r_{sm} < 2.3 \text{ \AA}$, $r_{lg} = 60 \text{ \AA}$) enables the two-pore model to achieve a slightly faster response. However, this response is still much slower than that predicted using models based on irreversible thermodynamics. It is possible that extending the pore theory model to three or more different pore sizes will enable the model to achieve more reasonable plasma volume estimates. The models based on irreversible thermodynamics already predict reasonable plasma volume responses, however, so the complexity of a 3-or-more-pore model does not appear to be warranted.

SUMMARY

The Kedem-Katchalsky equations³ make three assumptions which might restrict their use for describing transcapillary flux: 1) that the membrane is sufficiently thin to express concentration gradients in discrete form, 2) that the solutions on either side of the membrane are ideal, and 3) that the capillary wall is homogeneous. Several investigators have attempted to remedy these limitations by reworking the Kedem-Katchalsky equations for the more general case of a relatively thick membrane (Patlak model⁴), non-ideal solutions (Katz model⁵), and capillary wall nonhomogeneity (pore theory models⁶). The results of comparisons in the previous section show, however, that plasma volume predictions, generated by models incorporating different transcapillary flux equations, were indistinguishable. Thus, the Kedem-Katchalsky equations, when incorporated into a simple two-compartment model, are as effective as more complex models for describing the plasma volume response to hemorrhage and resuscitative fluid administration.

REFERENCES

1. Starling EH. On the absorption of fluids from the connective tissue spaces. *J Physiol (London)* 1896; 19:312-326.
2. Landis, EM. Micro-injection studies of capillary permeability II. The relation between capillary pressure and the rate at which fluid passes through the walls of single capillaries. *Am J Physiol* 1927; 82:217-238.
3. Kedem O, Katchalsky A. Thermodynamic analysis of the permeability of biological membranes to non-electrolytes. *Acta Biochem Biophys* 1958; 27:229-246.
4. Patlak CS, Goldstein DA, Hoffman JF. The flow of solute and solvent across a two-membrane system. *J Theor Biol* 1963; 5:426-442.
5. Katz, MA. New formulation of water and macromolecular flux which corrects for non-ideality: theory and derivation, predictions, and experimental results. *J Theor Biol* 1985; 112:369-401.
6. Curry FE. Mechanics and thermodynamics of transcapillary exchange. In: *Handbook of Physiology; Section 2, Volume 4, Part 1*. Bethesda, MD: American Physiological Society, 1974; 309-374.
7. Onsager L. Reciprocal relations in irreversible processes. *Phys Rev* 1931; 38:2255-2279.
8. Staverman, AJ. The theory of measurement of osmotic pressure. *Rec Trav Chim* 1951; 70:344-352.
9. Richardson IW. Some remarks on the Kedem-Katchalsky equations for non-electrolytes. *Bull Math Biophys* 1970; 32:237-247.
10. Axel B. Flow limits of Kedem-Katchalsky equations for fluid flux. *Bull Math Biol* 1976; 38:671-674.
11. Mikulecky DC. A simple network thermodynamic model for series-parallel coupled flows: II. The nonlinear theory with applications to coupled solute and volume flow in a series membrane. *J Theor Biol* 1977; 69:511-541.
12. Pappenheimer JR. Passage of molecules through the capillary walls. *Physiol. Rev.* 1953; 33:387-423.

13. Anderson JL, Malone DM. Mechanism of osmotic flow in porous membranes. *Biophys J* 1974; 14:957-983.
14. Faxen H. About T. Bohlin's paper: on the drag of rigid spheres moving in a viscous liquid inside cylindrical tubes. *Kolloid Z* 1959; 167:146.
15. Brenner H, Gaydos LJ. The constrained Brownian movement of spherical particles in cylindrical pores of comparable radius. Models of the diffusive and convective transport of solute molecules in membranes and porous media. *J. Colloid Interface Sci* 1977; 58:312-356.
16. Harper HA. Review of Physiological Chemistry. Los Altos, CA: Lange Med Pub, 1969; 533-535.
17. Landis EM, Pappenheimer JR. Exchange of substances through capillary walls. In: *Handbook of Physiology; Section 2, Volume 2*. Bethesda, MD: American Physiological Society. 1963; 961-1034.
18. Renkin EM. Transport pathways and processes. In: *Endothelial Cell Biology*; N. Simionescu and M. Simionescu, eds. Plenum Pub Corp, 1988; 51-68.
19. Renkin EM. Capillary transport of macromolecules: pores and other endothelial pathways. *J Appl Physiol* 1985; 58(2):315-325.
20. Dubick MA, Pfeiffer JW, Clifford CB, Runyon DE, Kramer GC. Comparison of intraosseous and intravenous delivery of hypertonic saline/dextran in anesthetized, euvoletic pigs. *Ann Emer Med* 1992; 21: 498-503.

Table 1. Initial conditions and parameter values for 2-compartment (vascular and interstitial) model.

<u>blood compartment</u>	
Blood Volume (BV)	70 ml/kg
Plasma Volume (PV)	38.5 ml/kg
Plasma NaCl Concentration ($C_{s,P}$)	0.0093 g/ml
Plasma Albumin Concentration ($C_{a,P}$)	0.045 g/ml
Plasma Globulin Concentration ($C_{g,P}$)	0.025 g/ml
Capillary Hydrostatic Pressure (P_C)	20 mm Hg
<u>interstitial-tissue compartment</u>	
Interstitial Volume (IV)	140 ml/kg
Tissue Volume (TV)	350 ml/kg
Interstitial NaCl Concentration ($C_{s,I}$)	0.0093 g/ml
Interstitial Albumin Concentration ($C_{a,I}$)	0.016 g/ml
Interstitial Globulin Concentration ($C_{g,I}$)	0.0 g/ml
Interstitial Hydrostatic Pressure (P_I)	-0.223 mm Hg

Table 2. Parameter values for models based on irreversible thermodynamics.

<u>assumed values</u>	
σ_s	0.109
σ_a	0.94
σ_g	1.0
k_s	$35.71 \text{ ml} \cdot \text{kg}^{-1} \cdot \text{min}^{-1}$
ν	$100 \times 10^{-8} \text{ m}$
<u>calculated values</u>	
L_p	$0.0612 \text{ ml} \cdot \text{kg}^{-1} \cdot \text{min}^{-1} \cdot \text{mm Hg}^{-1}$
k_a	$0.0103724 \text{ ml} \cdot \text{kg}^{-1} \cdot \text{min}^{-1}$
ω_a	$2.238 \times 10^{-5} \text{ g} \cdot \text{kg}^{-1} \cdot \text{min}^{-1} \cdot \text{mm Hg}^{-1}$

Table 3. Pore theory model parameter values for a system with two pore sizes, large (subscript lg) and small (subscript sm).

<u>assumed values</u>	
r_{sm}	$40 \times 10^{-8} \text{ m}$
r_{lg}	$200 \times 10^{-8} \text{ m}$
r_s	$10 \times 10^{-8} \text{ m}$
r_a	$36 \times 10^{-8} \text{ m}$
r_g	$56 \times 10^{-8} \text{ m}$
<u>calculated values</u>	
$k_{v,sm}$	$2.252 \times 10^{-9} \text{ ml} \cdot \text{kg}^{-1} \cdot \text{min}^{-1}$
$k_{v,lg}$	$9.970 \times 10^{-7} \text{ ml} \cdot \text{kg}^{-1} \cdot \text{min}^{-1}$
$k_{s,sm}$	$5.602 \times 10^{-12} \text{ ml} \cdot \text{kg}^{-1} \cdot \text{min}^{-1}$
$k_{s,lg}$	$1.409 \times 10^{-10} \text{ ml} \cdot \text{kg}^{-1} \cdot \text{min}^{-1}$
$k_{a,sm}$	$0.0 \text{ ml} \cdot \text{kg}^{-1} \cdot \text{min}^{-1}$
$k_{a,lg}$	$4.0183 \times 10^{-12} \text{ ml} \cdot \text{kg}^{-1} \cdot \text{min}^{-1}$
$\sigma_{s,sm}$	0.01055
$\sigma_{s,lg}$	0.0005229
$\sigma_{a,sm}$	0.9401
$\sigma_{a,lg}$	0.1073
$\sigma_{g,sm}$ and $\sigma_{g,lg}$	1.0
$\chi_{s,sm}$	0.9894
$\chi_{s,lg}$	0.9995
$\chi_{a,sm}$	0.0598
$\chi_{a,lg}$	0.8927
n_{sm}	11270160
n_{lg}	1111

Table 4. Flow-averaged parameter values for the one-pore model

k_v	0.0264855 ml·kg ⁻¹ ·min ⁻¹
k_s	6.32948x10 ⁻⁵ ml·kg ⁻¹ ·min ⁻¹
k_a	4.464988x10 ⁻⁹ ml·kg ⁻¹ ·min ⁻¹
σ_s	0.0103229
σ_a	0.9053186
σ_g	1.0

Box 1. Landis-Starling Equation

<u>equation</u>	<u>assumptions</u>
$J_v = k[(P_C - P_I) - (\Pi_C - \Pi_I)]$	Membrane is: 1) Freely permeable to small solutes 2) Non-permeable to proteins. Π represents protein oncotic pressure

Box 2. Kedem-Katchalsky Equations extended to a system of multiple, non-interacting solutes.

<u>equations</u>	<u>assumptions</u>
$J_v = k_v[\Delta P - \sum \sigma_s \Delta \Pi_s]$ $J_s = k_s \Delta C_s + (1 - \sigma_s) J_v \hat{C}_s$ $\hat{C}_s = \frac{\Delta C_s}{\Delta \ln(C_s)}$	Constant T and P Negligible solute volume fractions Thin membrane Ideal solutions Constant partial molar volumes

Box 3. Patlak Equations extended to a system of multiple, non-interacting solutes.

<u>equations</u>	<u>assumptions</u>
$J_v = k_v [\Delta P - \sum \sigma_s \Delta \Pi_s]$ $J_s = -k_s w \frac{dC_s}{dx} + (1 - \sigma_s) J_v C_s$	Constant T and P Negligible solute volume fractions Ideal solutions Constant partial molar volumes Homogeneous membrane L_p , ω_s , and σ_s are independent of C_s

Box 4. Continuous model with considerations for non-ideality extended to a system of multiple, non-interacting solutes.

<u>equations</u>	<u>assumptions</u>
$J_v = k_v [\Delta P - \sum \sigma_s \Delta \Pi_s]$ $J_s = -\omega_s w \frac{d\Pi_s}{dx} + (1 - \sigma_s) J_v C_s$	Constant T and P Constant partial molar volumes Homogeneous membrane

Box 5. Basic pore theory model extended to a system of multiple, non-interacting solutes.

<u>equations</u>	<u>assumptions</u>
$J_{v,p} = k_{v,p} [\Delta P - \sum \sigma_{s,p} \Delta \Pi_s]$	Non-interacting solute molecules Navier-Stokes flow Cylindrical pore Solutes do not affect solvent flow
$J_{s,p} = -\omega_{s,p} w \frac{d\Pi_s}{dx} + \chi_{s,p} C_s J_{v,p}$	
$k_{v,p} = \frac{\pi r_p^4}{8\eta w}$	
$\sigma_{s,p} = (1 - (1 - \lambda_{s,p})^2)^2$	
$\omega_{s,p} = A_{s,p} \left(\frac{f_{s,p}}{N_A 6\pi\eta r_s w} \right)$	
$\chi_{s,p} = (1 - \lambda_{s,p})^2 [2 - (1 - \lambda_{s,p})^2]$	

Box 6. Discrete, ideal pore theory model.

<u>equations</u>	<u>assumptions</u>
$J_{v,p} = k_{v,p} [\Delta P - \sum \sigma_{s,p} \Delta \Pi_s]$	Non-interacting solute molecules
$J_{s,p} = k_{s,p} \Delta C_s + \chi_{s,p} \hat{C}_s J_{v,p}$	Navier-Stokes flow
$k_{v,p} = \frac{\pi r_p^4}{8 \eta w}$	Cylindrical pore
$\sigma_{s,p} = (1 - (1 - \lambda_{s,p})^2)^2$	Solutes do not affect solvent flow
$k_{s,p} = A_{s,p} \left(\frac{f_{s,p} RT}{N_A 6 \pi \eta r_s w} \right)$	Ideal solutions
$\chi_{s,p} = (1 - \lambda_{s,p})^2 [2 - (1 - \lambda_{s,p})^2]$	Thin membrane

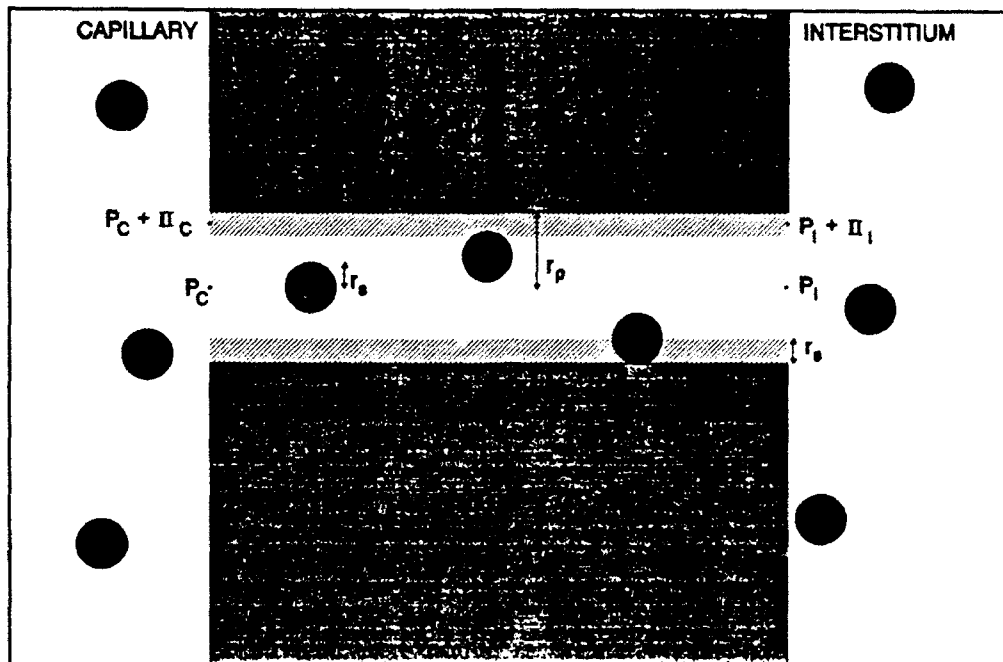


Figure 1. Pore transport model similar to that described by Anderson and Malone¹³.

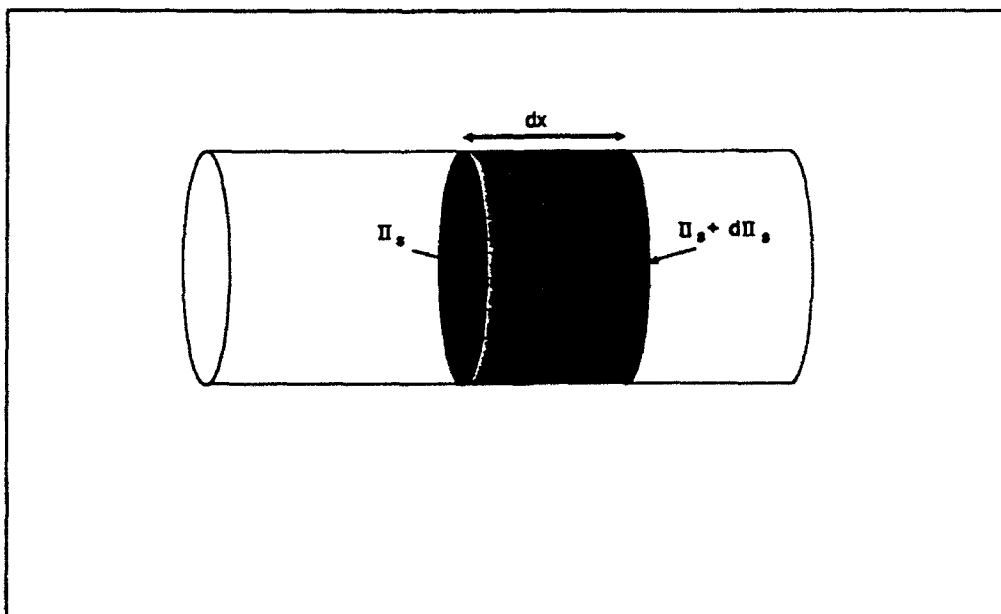


Figure 2. Hydrodynamic model for diffusion (adapted from Curry⁶).

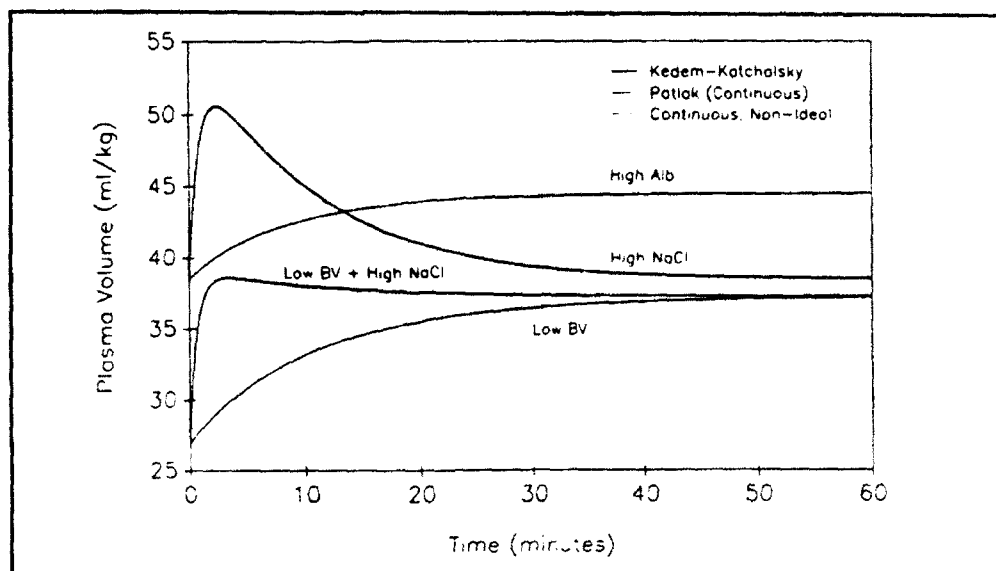


Figure 3. Plasma volume predictions generated by the three models based on irreversible thermodynamics.

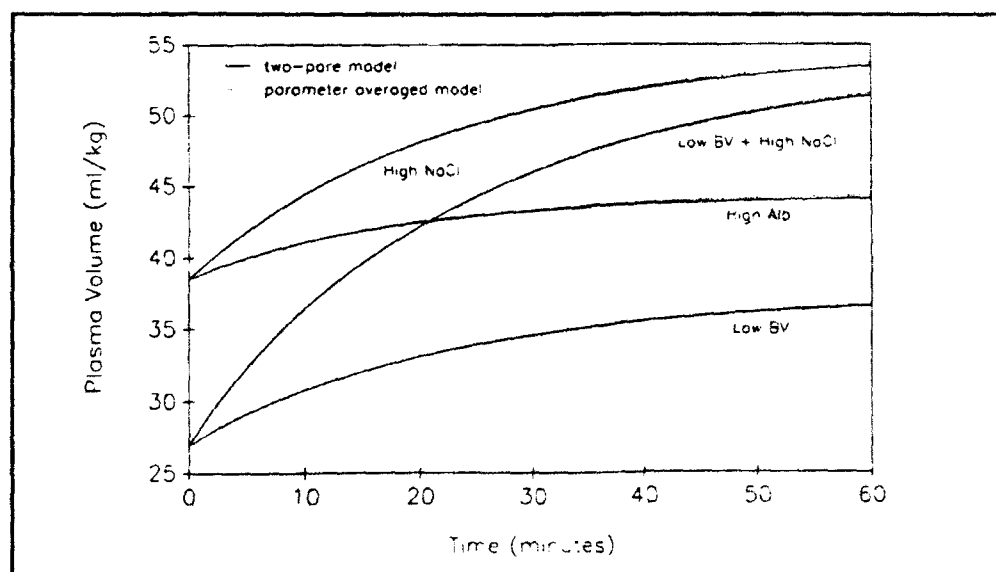


Figure 4. Plasma volume predictions generated by the two-pore and parameter-averaged models.

OFFICIAL DISTRIBUTION LIST

Commander

US Army Medical Research
& Development Command
ATTN: SGRD-RMS/Mrs. Madigan
Fort Detrick, MD 21701-5012

Defense Technical Information Center
ATTN: DTIC/DDAB (2 copies)
Cameron Station
Alexandria, VA 22304-6145

Office of Under Secretary of Defense
Research and Engineering
ATTN: R&AT (E&LS), Room 3D129
The Pentagon
Washington, DC 20301-3080

DASG-AAFJML
Army/Air Force Joint Medical Library
Offices of the Surgeons General
5109 Leesburg Pike, Room 670
Falls Church, VA 22041-3258

HQ DA (DASG-ZXA)
WASH DC 20310-2300

Commandant
Academy of Health Sciences
US Army
ATTN: HSHA-CDM
Fort Sam Houston, TX 78234-6100

Uniformed Services University of
Health Sciences
Office of Grants Management
4301 Jones Bridge Road
Bethesda, MD 20814-4799

US Army Research Office
ATTN: Chemical and Biological
Sciences Division
PO Box 12211
Research Triangle Park, NC 27709-2211

Director
ATTN: SGRD-UWZ-L
Walter Reed Army Institute of Research
Washington, DC. 20307-5100

Commander
US Army Medical Research Institute
of Infectious Diseases
ATTN: SGRD-ULZ-A
Fort Detrick, MD 21701-5011

Commander
US Army Medical Bioengineering Research
and Development Laboratory
ATTN: SGRD-UBG-M
Fort Detrick, Bldg 568
Frederick, MD 21701-5010

Commander
US Army Medical Bioengineering
Research & Development Laboratory
ATTN: Library
Fort Detrick, Bldg 568
Frederick, MD 21701-5010

Commander
US Army Research Institute
of Environmental Medicine
ATTN: SGRD-UE-RSA
Kansas Street
Natick, MA 01760-5007

Commander
US Army Research Institute of
Surgical Research
Fort Sam Houston, TX 78234-6200

Commander
US Army Research Institute of
Chemical Defense
ATTN: SGRD-UV-AJ
Aberdeen Proving Ground, MD 21010-5425

Commander
US Army Aeromedical Research
Laboratory
Fort Rucker, AL 36362-5000

AIR FORCE Office of Scientific
Research (NL)
Building 410, Room A217
Bolling Air Force Base, DC 20332-6448

Strughold Aeromedical Library
Armstrong Laboratory/DOKOD
2511 Kennedy Dr.
Brooks AFB TX 78235-5122

Head, Biological Sciences Division
OFFICE OF NAVAL RESEARCH
800 North Quincy Street
Arlington, VA 22217-5000

Commander
Naval Medical Command-02
Department of the Navy
Washington, DC 20372-5120